

Toxicology Research

Accepted Manuscript



This is an *Accepted Manuscript*, which has been through the Royal Society of Chemistry peer review process and has been accepted for publication.

Accepted Manuscripts are published online shortly after acceptance, before technical editing, formatting and proof reading. Using this free service, authors can make their results available to the community, in citable form, before we publish the edited article. We will replace this *Accepted Manuscript* with the edited and formatted *Advance Article* as soon as it is available.

You can find more information about *Accepted Manuscripts* in the [Information for Authors](#).

Please note that technical editing may introduce minor changes to the text and/or graphics, which may alter content. The journal's standard [Terms & Conditions](#) and the [Ethical guidelines](#) still apply. In no event shall the Royal Society of Chemistry be held responsible for any errors or omissions in this *Accepted Manuscript* or any consequences arising from the use of any information it contains.



Hydroxylated-graphene quantum dots induce cells senescence in both p53-dependent and -independent manner

Xin Tian[†],^a Bei-Bei Xiao[†],^a Anqing Wu,^a Lan Yu,^c Jundong Zhou,^d Yu Wang,^b Nan Wang,^a Hua Guan^{††b} and Zeng-Fu Shang^{††a}

Received 00th January 20xx,
Accepted 00th January 20xx

DOI: 10.1039/x0xx00000x

www.rsc.org/toxicology

The numerous particular chemical/physical properties make graphene quantum dots (GQDs) attractive for various biomedical applications such as drug delivery, bioimaging and tumor photodynamic therapy (PDT). In present study, the critical roles of hydroxyl-modified GQDs (OH-GQDs) on lung carcinoma A549 (wild type p53) and H1299 (p53-null) cells were investigated. Our data showed that medium concentration (50 µg/mL) of OH-GQDs significantly decreased the viability of A549 and H1299 cells. OH-GQDs treatment enhanced intracellular reactive oxygen species (ROS) generation. Furthermore, we found that treatment with ROS scavenger N-acetylcysteine (NAC) at least partially abolished the cytotoxicity effect of OH-GQDs on A549 and H1299 cells. Hydroxylated GQDs lead to G0-G1 arrest and cells senescence. Signal pathway analysis revealed that OH-GQDs activated the expression of p21 in both p53-dependent and -independent manner. Consistent with this, OH-GQDs could also inhibit the phosphorylation of Rb in both A549 and H1299 cells. These findings provide valuable information for the consideration of biomedical application of GQDs in the future.

Introduction

Graphene quantum dots (GQDs), as a new kind of zero-dimensional (0D) carbon material, are smaller than 100 nm in size and have the single-atom layer in thickness.^{1,2} Owing to their particular chemical/physical properties, GQDs have the great potential in various areas such as energy, electrochemical, environmental and biomedical applications.^{1,3-6} Among them, biomedical application is a new field and its biological safety has caught much attention in recent years. Due to its high water solubility and stability, GQDs has better biocompatibility when compared with other carbon-based nanomaterials.⁷ For instance, GQDs can serve as good vectors for drug or protein molecular delivery. Wang et al. found that without any pre-modification, GQDs could also efficiently deliver doxorubicin (DOX) into the nucleus and significantly increase the binding affinity of DOX to DNA, thereby improve

its DNA cleavage activity and cytotoxicity even in drug resistant cancer cells.⁸ GQDs exhibit higher potency in drug delivery and cancer therapy than graphene oxide (GO) or other nanoparticles.^{7,8} In addition, based on the dependence of the binding of Dox with GQDs on pH, GQDs can be designed as the novel pH-sensitive drug delivery system to improve drug releasing specifically in cancer cells which are slightly more acidic than normal tissue and blood.⁹ Recently, Ge and colleagues revealed that GQDs is a novel photodynamic therapy agent through producing singlet oxygen in a multistate sensitization process.¹⁰ The excellent luminescent properties of GQDs also enable them to act as good fluorescent probes for bioimaging simultaneously.^{11,12} Despite these studies have proposed that GQDs seem to be the bio-friendly material,¹³ its biomedical application will still be limited unless its potential toxicity is carefully assessed.

Several recent studies have been performed to evaluate the in vivo and in vitro toxicity of GQDs in different biosystems. Wu's study demonstrated that GQDs exhibit much lower cytotoxicity in gastric and breast cancer cells when compared with micrometer-size GO.¹⁴ Furthermore, Zhang's group found that GQDs with sizes vary from 3 to 5 nm have no obvious toxic effect on mice. The biodistribution experiment revealed no GQDs accumulation in main organs of mice.¹⁵ On the other hand, Qin and colleagues proved that GQDs could significantly enhance the generation of reactive oxygen species (ROS) and then lead to activation of inflammatory response through activating p38MAPK and NF-κB signaling pathway in macrophages.¹⁶ This study also revealed that GQDs result in autophagy which has been recognized as the effector and player in genotoxicants induced DNA damage response

^a School of Radiation Medicine and Protection, Medical College of Soochow University, Collaborative Innovation Center of Radiation Medicine of Jiangsu Higher Education Institutions, Suzhou, Jiangsu 215123, P.R. China. E-mail: zengfu.shang@suda.edu.cn.

^b Department of Radiation Toxicology and Oncology, Beijing Key Laboratory for Radiobiology (BKLRB), Beijing Institute of Radiation Medicine, Beijing 100850, P. R. China. E-mail: ghsh@163.com.

^c Division of Molecular Radiation Biology, Department of Radiation Oncology, University of Texas Southwestern Medical Center at Dallas, Dallas, Texas 75390, USA.

^d Suzhou Cancer Center Core Laboratory, Nanjing Medical University Affiliated Suzhou Hospital, Suzhou, Jiangsu 215001, P.R. China.

[†] These authors contributed equally to this work.

^{††} Shang ZF and Guan H are Corresponding authors

See DOI: 10.1039/x0xx00000x

(DDR).¹⁷ Consistent with this report, GQDs also induce ROS generation in NIH-3T3 cells, through which GQDs increase the expression of DNA damage response proteins, including Rad51, OGG1 and p53.¹⁸ These results indicated that GQDs are the potential genotoxic agents. In response to DNA damage, the cell will activate DNA damage response, in which the cells stop cell cycle progression providing enough time to repair DNA lesions. If the damage is irreparable, cells will ultimately launch cell death program to prevent the genomic instability which is highly correlated with pathophysiology and disease, such as cancer.¹⁹ Therefore, on the basis of these studies, the toxicity of GQDs is still critical obstacle for its wide application in biomedical fields.

The surface modification of nanomaterials can change their characteristics. For instance, partially hydroxylated and carboxylated GQDs exhibit a half-metallic state under almost same electric-field intensity.²⁰ The modifications also provide the platform to conjugate with different functional molecules to facilitate greater biocompatibility. Yuan et al. compared the toxic effect of GQDs with different modified groups (NH₂, COOH and CO-N (CH₃)₂) and found that all of these modified GQDs has good biocompatibility even in high concentration.²¹ However, Wang et al. analyzed the toxicity of nitrogen-doped graphene quantum dots (N-GQDs) in red blood cells (RBCs) and found that N-GQDs disturb the order and conformation of lipid and lead to the formation of echinocytes.²² Here, we studied the cytotoxicity of hydroxyl-modified GQDs (OH-GQDs) and demonstrated that 50 µg/mL OH-GQDs significantly inhibit the viability of human lung carcinoma cells (A549 and H1299). OH-GQDs could also enhance the ROS generation and block the cell cycle at G₀-G₁ phase. Finally, OH-GQDs induce cells senescence but not apoptosis (data not shown) through promoting p21 expression and inhibiting phosphorylation of Rb in both p53-dependent and -independent manners. Our study will provide valuable information for GQDs toxicity assessment.

Materials and Methods

Material Characterization

The hydroxyl-modified GQDs were purchased from XFNANO Materials Tech Co. (Nanjing, Jiangsu, China). Physical properties of GQDs were characterized by various techniques, including transmission electron microscopy (TEM), dynamic light scattering (DLS) and zeta potential analysis. The diameter of GQDs was observed by TEM (FEI, Tecnai G2). Hydrodynamic diameter of GQDs in PBS buffer was analyzed by a DLS instrument. Zeta potential for GQDs was conducted using a particle analyzer (Malvern, Zetasizer Nano-ZS).

Cell culture and treatment

The human lung carcinoma cell lines A549 and H1299 were kindly provided by Dr. Hongying Yang at Medical College of Soochow University, Suzhou, Jiangsu, China, and grown in RPMI 1640 medium with 10% FBS (HyClone, Hudson, NH, USA) at 37°C with 5% CO₂. Cells were treated with various

concentrations of hydroxyl-modified GQDs (XFNANO Materials Tech Co, Nanjing, Jiangsu, China) for different time.

CCK-8 assay analysis of cell viability

A549 and H1299 cells were cultured in a 96-well plate at density of 5×10^3 cells/well. 24 hours later, cells were treated with 12.5, 25, 50 and 100 µg/mL hydroxyl-modified GQDs for 24 and 48 hours. The negative control groups were incubated with equal amount of PBS. The CCK-8 assay was performed according to the instructions. In brief, 10 µL CCK-8 solution (Beyotime, Shanghai, China) was added in each well and incubated for 1 hour at 37°C. Absorbance was monitored at 450 nm and normalized to controls.

Cell cycle distribution analysis

A549 and H1299 cells were treated with 50 µg/mL OH-GQDs for 24 and 48 hours, respectively. Cells were harvested and then performed as previously described.²³

Measurement of intracellular ROS generation

A549 and H1299 cells were seeded into 60 mm² dish at a density of 1.5×10^5 mL⁻¹. 24 and 48 hours after 50 µg/mL OH-GQDs treatment, cells were incubated with 200 µL of 100 µM DCFH-DA (Sigma-Aldrich, St Louis, MO, USA) at 37°C with 5% CO₂ for 30 min. After the aspiration of the DCFH-DA, cells were harvested and the ROS probe was measured by flow cytometry. The data was presented as the average ROS intensity.

Senescence-associated β-galactosidase staining

Cells were treated with 50 µg/mL OH-GQDs for 24 and 48 hours and then fixed in 2% formaldehyde/0.2% glutaraldehyde for 5 min at room temperature. The fixed cells were washed twice with PBS and add β-galactosidase staining solution containing 20 mg/mL X-gal (Beyotime, Shanghai, China), cells were incubated for 6-10 hours at 37°C incubator without CO₂.

Immunoblotting and Immunofluorescence analysis

Whole-cell lysate preparation and western blotting were mentioned in our published paper.²⁴ The primary antibodies used for western blotting analysis are anti-p21 (1: 1000, Cell Signaling Technology, Danvers, MA, USA) antibody, anti-p53 (1:1000, Cell Signaling Technology, Danvers, MA, USA) antibody, anti-PIG3 (1:1000, Santa Cruz, California, CA, USA) antibody, anti-pRb, Rb (1:1000, Cell Signaling Technology, Danvers, MA, USA) antibodies and GAPDH (1:1000, Santa Cruz, California, CA, USA) antibody. Secondary antibodies were the goat anti-rabbit and -mouse IgG-horseradish peroxidase conjugated (Pierce, Rockford, IL).

For immunofluorescence assay, A549 and H1299 cells were seeded on slide covers in 35 mm² dishes. Cells were treated with 50 µg/mL OH-GQDs for 24 and 48 hours and then fixed with 4% (v/v) paraformaldehyde. The immunofluorescent staining were performed as previously described.²⁵ In brief, the fixed cells were blocked in blocking buffer (2% BSA/PBS) for 30 min at room temperature. Cells were incubated with an anti-p21 (1: 200, Cell Signaling Technology, Danvers, MA, USA) antibody and an anti-p53 (1: 200, Cell Signaling Technology, Danvers, MA, USA) antibody for 4 hours at room temperature.

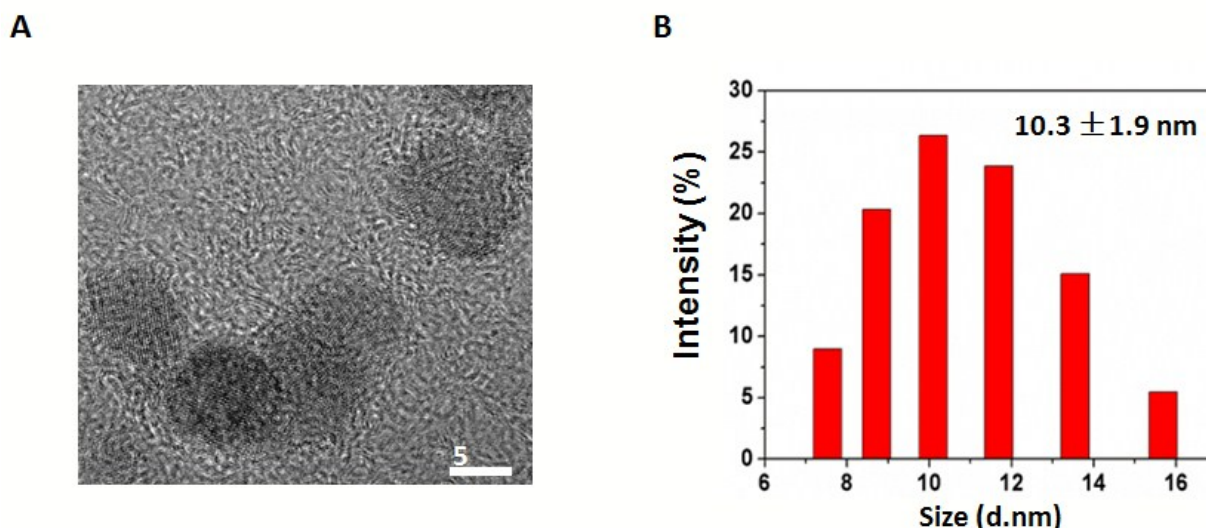


Fig. 1 Characterization of GQD. (A) Typical TEM image of GQD (Scale 5nm). (B) The hydrodynamic diameter of GQD.

The cells were then incubated with Alexa-568- and Alexa-488-conjugated secondary antibodies (BD Pharmingen, San Diego, CA, USA) for 1 h. Nucleus were stained with 100 $\mu\text{g}/\text{mL}$ DAPI in mounting solution. Confocal immunofluorescence microscopy was performed using an LSM 510 laser-scanning confocal microscope (Carl Zeiss, Oberkochen, Germany).

Statistical analysis

Data is presented as the mean \pm SD of at least three independent experiments. The results were tested significance using the unpaired Student's t test.

Results

Characteristics and morphology of OH-GQDs

The hydroxylated GQDs were obtained commercially. GQDs were monodispersed with average diameter of 5.6 ± 1.1 nm, which was calculated by measuring at least 100 GQDs under transmission electron microscopy (TEM). We used the dynamic light scattering (DLS) method to measure their hydrodynamic diameters. As shown in Figure 1B, the hydrodynamic diameter of GQD is 10.3 ± 1.9 nm. The GQDs were negative charged, evidenced by -5.0 mV as the zeta potential, which was analyzed using a particle analyzer. GQDs were ultrasonic 5 min and vortex 1 min before use.

The effect of hydroxylated GQDs on cellular viability of lung carcinoma cells

Wang et al. reported that GQDs could induce the expression of p53, which is a tumor suppressor and is correlated with DNA damage response.¹⁸ Here, we determined whether hydroxylated GQDs have different effect of proliferation and cell cycle progression on cells with different p53 gene status. Human lung carcinoma A549 (wild type p53) and H1299 (p53-null) cells were incubated with different concentration (12.5,

25, 50 and 100 $\mu\text{g}/\text{mL}$) of hydroxylated GQDs for 24 and 48 hours. As shown in Figure 2 A and B, a significant decrease of cell proliferation was induced by OH-GQDs in a concentration dependent manner in both cell lines. The A549 cells viability was found to be 76.8% and 65.2% when cells were exposed to 50 and 100 $\mu\text{g}/\text{mL}$ OH-GQDs for 24h, and the cells viability decreased to 58.9% and 31.7% when cells were incubated with 50 and 100 $\mu\text{g}/\text{mL}$ OH-GQDs for 48h, respectively. The cells viability for H1299 cells was reduced to 86.9% and 64% when the cells were exposed to 50 and 100 $\mu\text{g}/\text{mL}$ OH-GQDs for 24h, and to 88.4% and 34.1% when the cells were exposed to 50 and 100 $\mu\text{g}/\text{mL}$ OH-GQDs for 48h (Figure 2A and B). We further treated A549 and H1299 cells with 50 $\mu\text{g}/\text{mL}$ hydroxylated GQDs for different time (24, 48, 72 and 96h), and cells proliferation speed was determined by cells counting. As Figure 2 C and D shown, 50 $\mu\text{g}/\text{mL}$ OH-GQDs almost totally inhibited the proliferation of A549 cells after 72h treatment. H1299 are still growing when exposed to 50 $\mu\text{g}/\text{mL}$ OH-GQDs, however, the proliferation speed significantly slowed down in OH-GQDs treated group when compared with control cells. These results indicated that hydroxylated GQDs have obvious cytotoxicity towards lung cancer cells in a concentration dependent manner.

Hydroxylation modified GQDs induced the accumulation of G0-G1 cells population of cell cycle

To further ascertain the effect of OH-GQDs on cell growth, the cell cycle distribution of A549 and H1299 cells were analyzed by flow cytometry. The A549 and H1299 cells were incubated with 50 $\mu\text{g}/\text{mL}$ OH-GQDs for 24 and 48 hours. OH-GQDs resulted in a significantly increased accumulation of G0-G1 population in both A549 and H1299 cells. The percentage of G0-G1 cells increased from 55.1% to 81.1% in A549 cells, and from 42.9% to 69.1% in H1299 cells after OH-GQDs treatment for 48 hours. Such data suggested that medium concentration of OH-GQDs was enough to induce robust G0-G1 cells

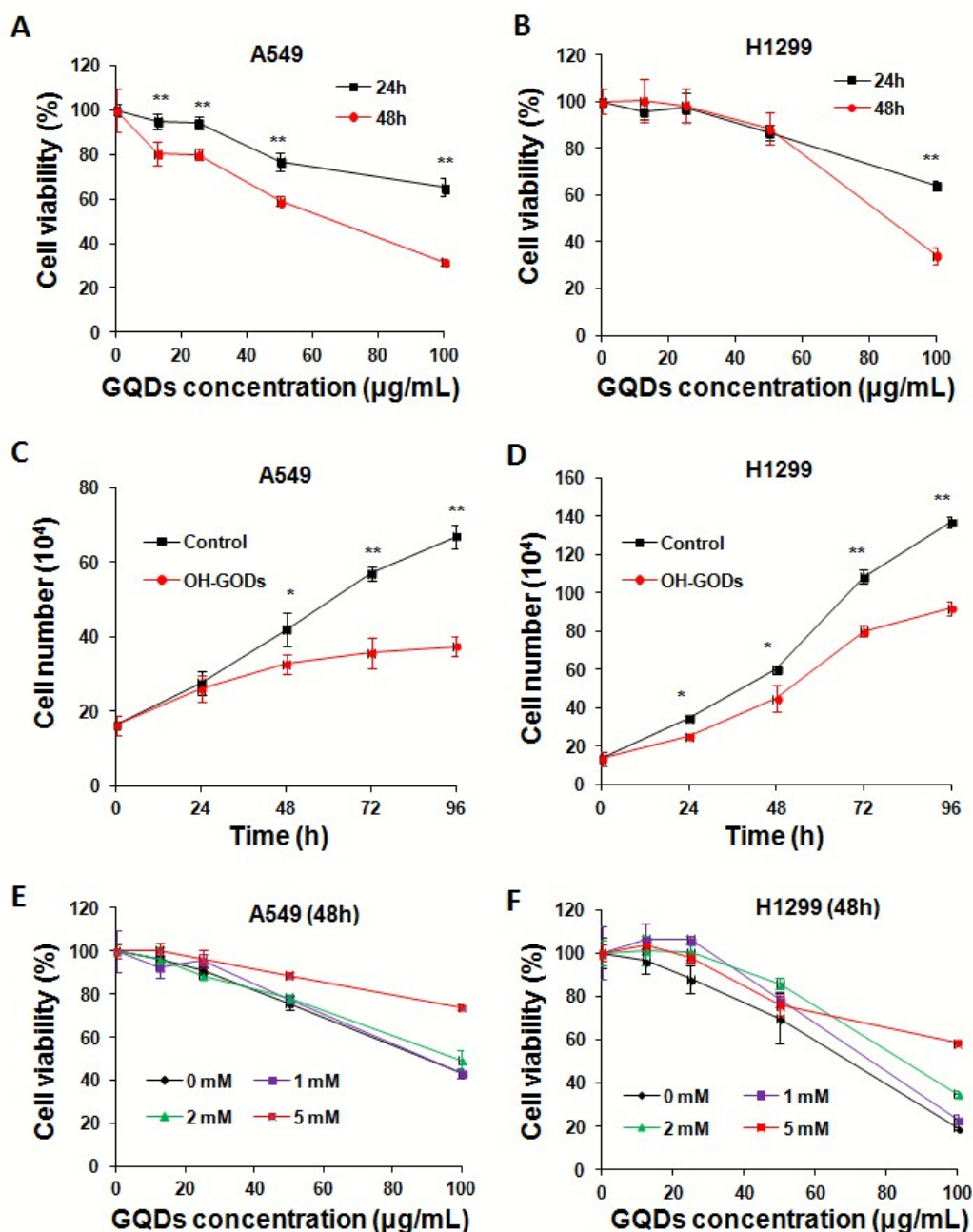


Fig. 2 Evaluation of cytotoxicity of hydroxyl-modified GQDs. (A, B) Cell viability after exposure to indicated concentration of OH-GQDs (12.5, 25, 50,100 µg/mL) for 24 and 48 hours, respectively. Data are expressed as mean ± standard deviation (S.D.), **p* < 0.05, ***p* < 0.01, *n* = 5. (C, D) 1.6×10^5 A549 cells and 1.4×10^5 H1299 cells were plated at day 0 and cells were treated or untreated with 50 µg/mL OH-GQDs for indicated time. Cell numbers were counted at indicated day to generate a growth curve. The data are the mean ± S.D. from three tests, ***p* < 0.01 compared with control group at the same time point. (E, F) A549 and H1299 cells were exposed to 50 µg/mL OH-GQDs, meanwhile, cells were treated with indicated concentration of ROS scavenger NAC (1, 2 and 5 mM) for 48 hours. Cell viability was determined by CCK-8 assay. The data are the mean ± S.D. from five tests.

accumulation through an unknown mechanism of cell cycle arrest, quiescence or senescence induction in both A549 and H1299 cells (Figure 3A, B).

OH-GQDs enhance ROS generation in A549 and H1299 cells

There are several groups have revealed that GQDs could promote the generation of ROS in different types of cells. To

further confirm the ROS generation of lung carcinoma cells after treated with OH-GQDs, the DCFH-DA measurement was performed. We treated A549 and H1299 cells with 50 µg/mL OH-GQDs for 24 and 48 hours. As shown in Figure 4, OH-GQDs treatment significantly increased the ROS levels in A549 cells 48 hours after exposure. H1299 cells exhibited higher basal

Toxicology Research Accepted Manuscript

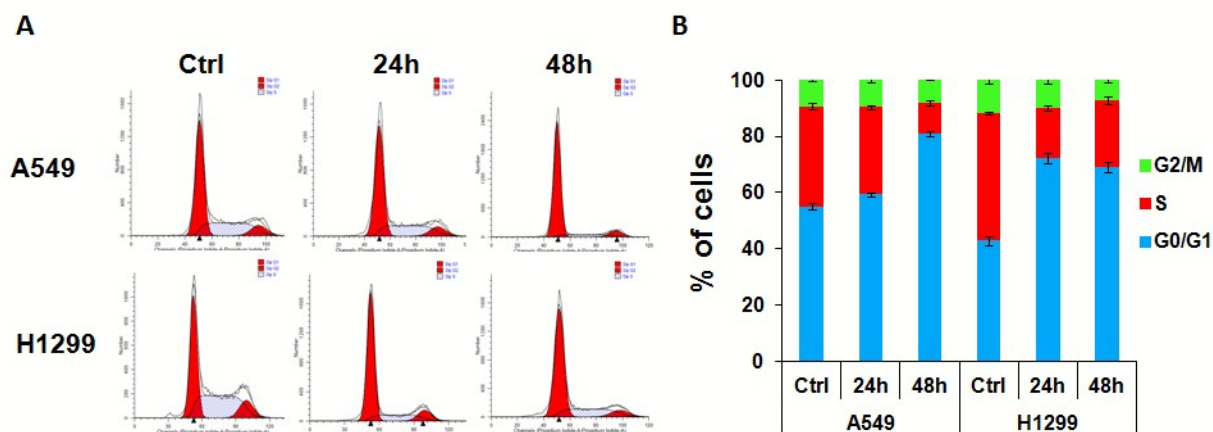


Fig. 3 Effect of hydroxylated GQDs on cell cycle distribution. (A, B) A549 and H1299 cells were treated with 50 $\mu\text{g}/\text{mL}$ OH-GQDs for 24 and 48 hours, cell cycle distributions of these groups were detected by flow cytometry assay. The data are the mean \pm S.D. from three tests.

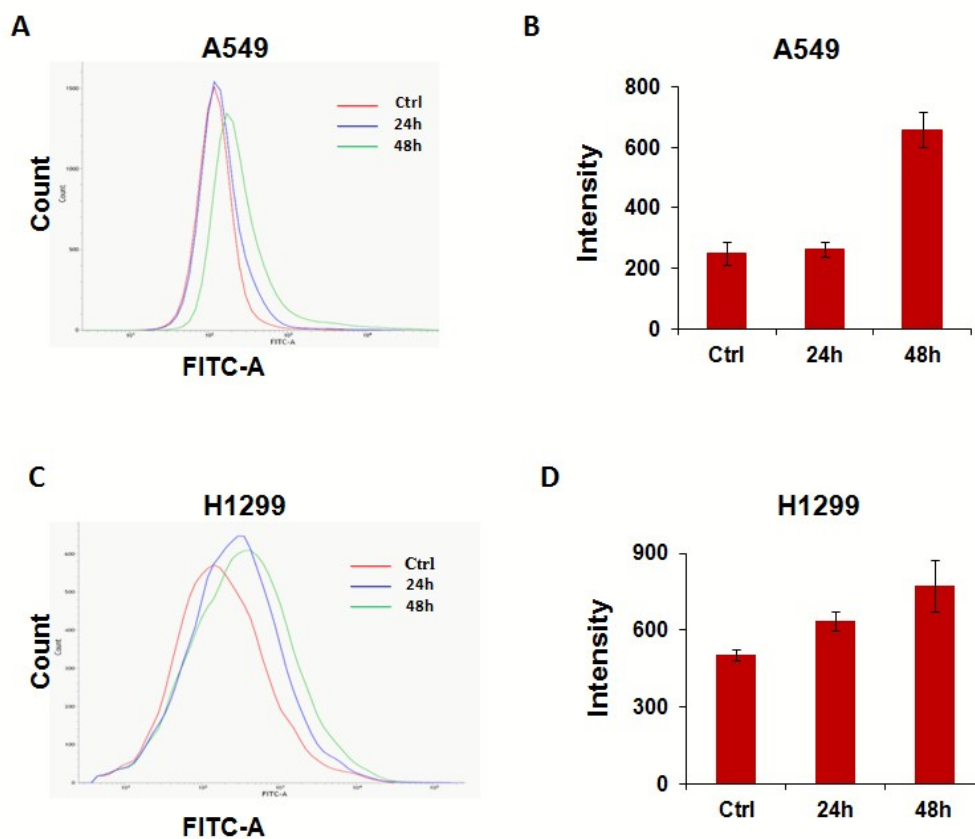


Fig. 4 Hydroxyl-modified GQDs enhanced the generation of ROS. A549 and H1299 cells were treated with 50 $\mu\text{g}/\text{mL}$ OH-GQDs for 24 and 48 hours, cells were then incubated with 200 μL of 100 μM DCFH-DA for another 30 min at 37 $^{\circ}\text{C}$. Cells were collected and detected using a 525-nm bandpass filter by flow-cytometric analysis. (A, C) Representative pictures of flow cytometry for the DCFH-DA probes. (B, D) Analysis by flow cytometry of the DCF+ incorporation rate in OH-GQDs treated or control groups of A549 and H1299 cells.

level of ROS and OH-GQDs could further enhance ROS generation.

To further determine whether ROS plays the essential role in OH-GQDs-induced cytotoxicity. Different concentration (1, 2 and 5 mM) of ROS scavenger N-acetylcysteine were incubated with A549 and H1299 cells which were exposed to 50 µg/mL OH-GQDs at the same time. As shown in Figure 2E and F, NAC significantly rescued the cell growth inhibited by OH-GQDs.

OH-GQDs induces senescence in lung carcinoma cells

Continuous generation of ROS can lead to cells permanently exit from cell cycle, which is known as cellular senescence. Hence, we investigated the effect of OH-GQDs on senescent phenotype in both A549 and H1299 cell lines. Senescence-associated beta-galactosidase (SA-β-gal) activity was detected using SA-β-gal staining. Figure 5 clearly showed that 50 µg/mL OH-GQDs treatment led to marked increase of senescence in both A549 and H1299 cells. Consistent with this result, we also found that OH-GQDs treated cells displayed an enlarged cell size which was recognized a marker of senescent cells (Figure 5).

Because p53-p21 pathway play an important role in ROS induced senescence, we therefore examined the expression levels of p53 and p21 in these cells using immunofluorescent staining and Western blotting assays. We found that OH-GQDs dramatically promoted the accumulation of p21 in A549 cells 48h after treatment, but don't affect the expression of another p53-induced gene, PIG3, which is reported to be correlated with p53-dependent apoptosis. Interestingly, OH-GQDs also

induced the expression of p21 in p53-deficient H1299 cells despite the signal was weaker comparing with the signal in p53-wt A549 cells, suggesting other upstream regulator also participates in OH-GQDs induced cell senescence (Figure 6). We have also observed that OH-GQDs inhibited the phosphorylation of Rb protein (Figure 6). These finding indicated that OH-GQDs induce ROS production, through which OH-GQDs activate p21 signal pathway in both p53-dependent and -independent manners. The activated p21 play an important role in mediating cell cycle arrest and inducing senescence (Figure 6C).

Discussion

Although the cytotoxicity of GQDs with or without modifications has been reported in a few recent studies, the conclusions are still contradictory.^{14, 16, 18, 21} Moreover, the effects of hydroxylated GQDs on biosystems have not been elucidated. Here, our study demonstrated that the OH-GQDs exhibit obvious cytotoxicity on lung carcinoma A549 and H1299 cells, which have different p53 gene status (Figure 2). Medium concentration of OH-GQDs (50 µg/mL) almost totally inhibit the cell growth in A549 (wild type p53) cells and can also dramatically slow down H1299 (p53 null) cells growth speed (Figure 2). p53 is one of the most studied tumor suppressor and plays an important role in genomic stability

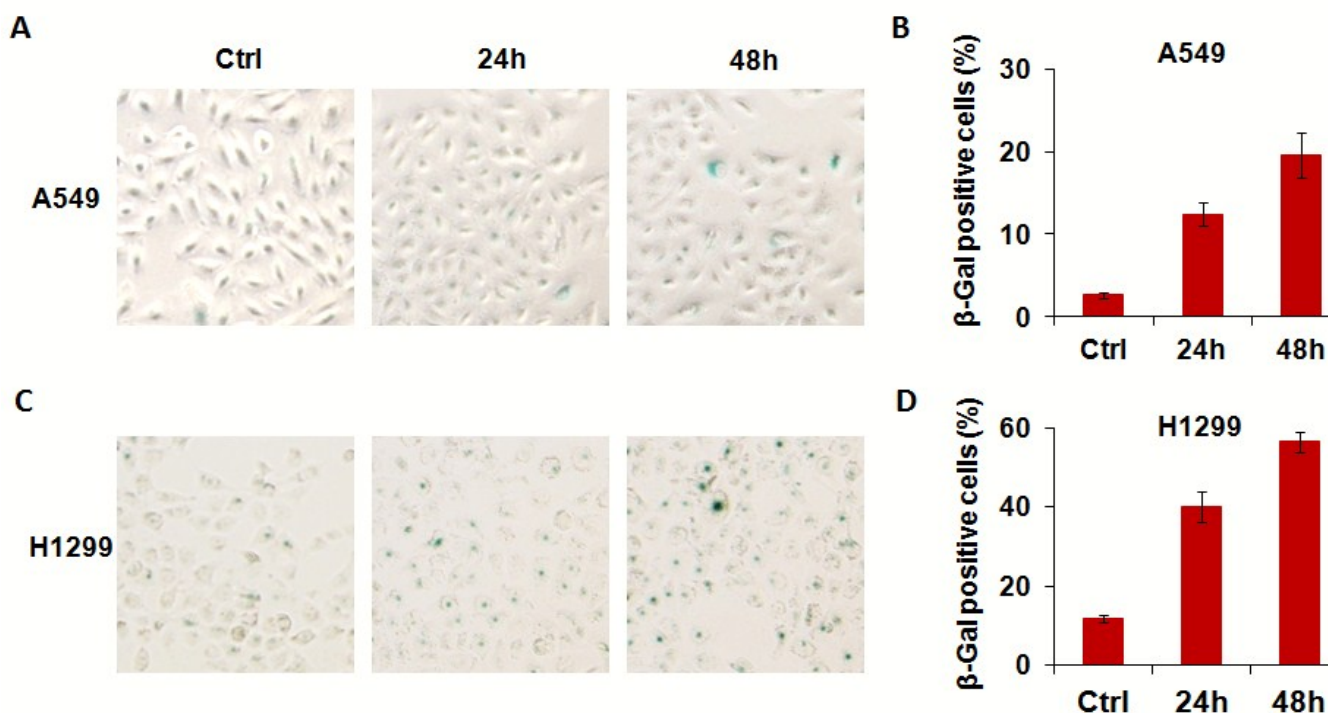


Fig. 5 Hydroxyl-modified GQDs induced cellular senescence in lung carcinoma cells. A549 and H1299 cells were treated with 50 µg/mL OH-GQDs for 24 and 48 hours and then stained with X-Gal. (A, C) Representative image of SA-βGal activity after 24 and 48 hours treatment. (B, D) Quantitative analysis of senescent cells. The data are presented as the means ± SD of three independent experiments.

maintenance through responding to various environmental stimuli.²⁶ Wang et al. revealed that GQDs could induce the expression of p53 in NIH-3T3 cells using flow cytometry analysis.¹⁸ In the present study, we didn't find the increased expression of p53 in hydroxylated GQDs-treated A549 cells using Western blotting method (Figure 6). However, we observed that OH-GQDs significantly promote the accumulation of p53 in the nucleus 24 and 48 hours after exposure (Figure 6A). As a transcription factor, nuclear

translocation of p53 is necessary for its binding with DNA and achieving its activation.²⁷ Therefore, our data indicated that OH-GQDs might contribute to p53 activation through facilitating p53 nuclear retention. Why unmodified GQDs enhance the expression of p53, whereas hydroxylation modified GQDs regulate the cellular localization of p53 remains an interesting questions.

In response to diverse stresses, activated p53 bind to DNA as a tetramer to transactivate or transrepress numerous target

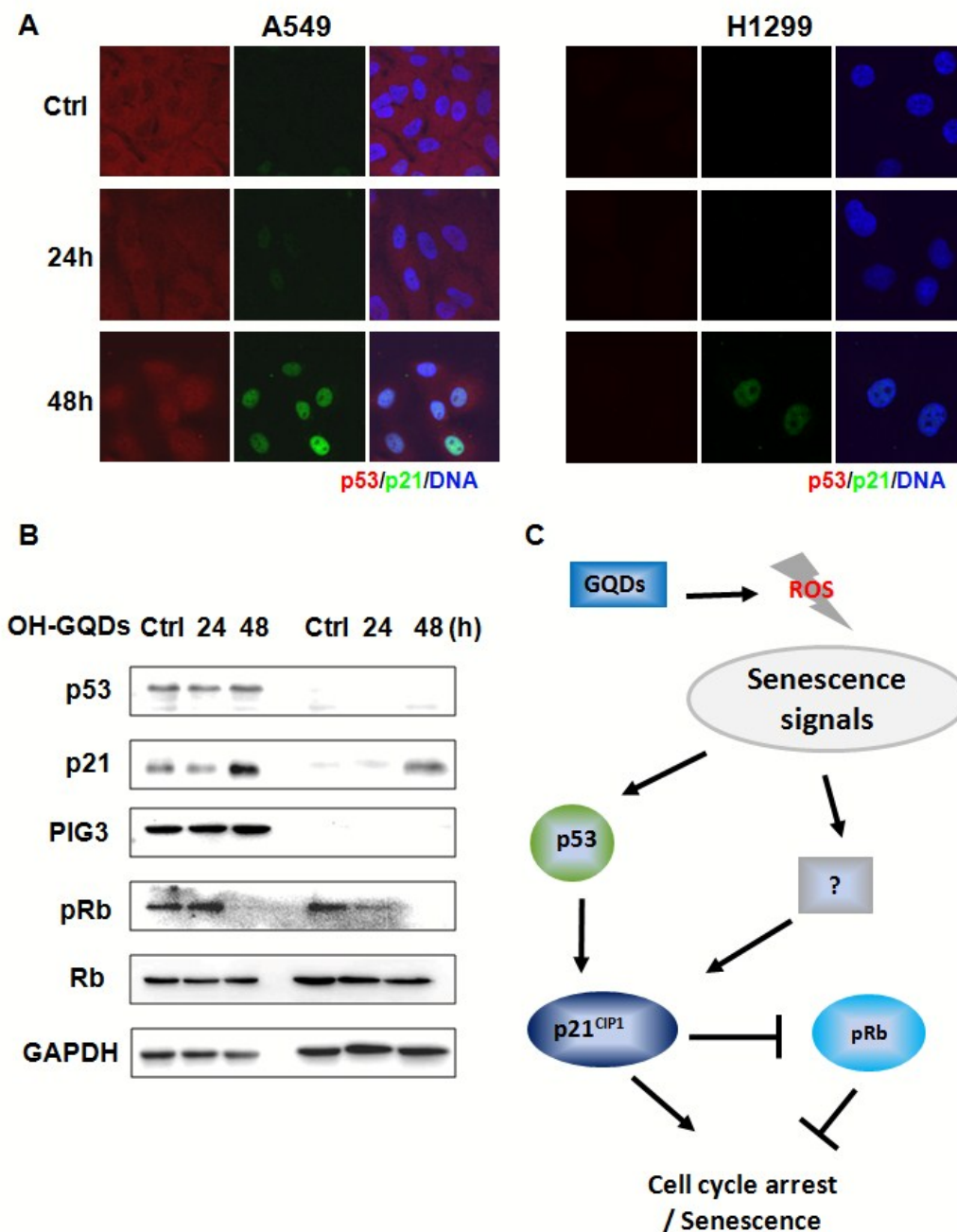


Fig. 6 Signaling pathway analysis after hydroxyl-modified GQDs treatment. A, A549 and H1299 cells were fixed 24 and 48 hours after exposure to 50 $\mu\text{g}/\text{mL}$ OH-GQDs and subjected to immunofluorescent analysis, the signal of p53 and p21 were detected. B, A549 and H1299 cells were lysed 24 and 48 hours after exposure to 50 $\mu\text{g}/\text{mL}$ OH-GQDs and subjected to Western blot analysis, the expression of p53, p21, Rb, phosphorylated Rb and PIG3 were determined. C, The work model of the effect of OH-GQDs on induction of cell cycle arrest and senescence through activation of p21, Rb signal pathways in both p53-dependent and -independent manner.

genes which involved in different cellular responses, including cell cycle arrest, cellular senescence and apoptosis.²⁸ p21 is one of p53-activated factors and was first discovered as a mediator of cell cycle arrest by inhibiting activity of cyclin-dependent kinase (CDK). Our results showed that OH-GQDs markedly induced the expression of p21 in A549 cells (Figure 6). Interestingly, we also observed the significantly increased expression of p21 in p53-null lung cancer H1299 cells after OH-GQDs treatment. In addition to p53, several other transcription factors can bind to p21 promoter to regulate p21 expression. For example, forkhead box A1/2 is required for p21 transcription in p53-null H1299 cells.²⁹ Chk2 can activate p21 transcription in p53-deficient breast cancer HaCaT and SK-BR-3 cells.³⁰ Furthermore, transcription factors including SP1,³¹ ATM,³² Brca1³³ and c-Myc³⁴ were demonstrated to involve in p21 activation even in p53 deficient cells. The potential signal pathways that participate in OH-GQDs-induced p21 activation in p53-null H1299 cells merit further exploration. Due to the important role of p21 in cell cycle arrest, we analyzed the cell cycle distribution of A549 and H1299 cells and discovered that treatment with 50 µg/mL OH-GQDs resulted in robust increased accumulation G0-G1 cells population in both of these two lung cancer cell lines used in this study (Figure 3). Together, our results indicated that OH-GQDs could halt cell cycle progression by activating the expression of p21 in both p53-dependent and -independent manner.

In addition to GQDs, several other nanoparticles have been shown to activate p21 signaling, most probably via induction of oxidative stress,³⁵ such as silica nanoparticles³⁶ and zinc oxide nanoparticles³⁷. Wang¹⁸ and Qin¹⁶ have shown that GQDs treatment increase the intracellular ROS generation. Consequently, our finding showed that OH-GQDs significantly promote ROS generation in lung carcinoma cells. Furthermore, we demonstrated that treatment of cells with NAC, a ROS scavenger, could at least partially protect cells against OH-GQDs mediated cytotoxicity (Figure 2E and F). p53 has both pro-oxidant and antioxidant properties in response to various stresses through activating different groups of downstream target genes. For example, p53 has been implicated in regulation of a subset of important antioxidant factors including glutathione peroxidase 1 (GPX1) and mitochondrial superoxide dismutase 2, suggesting it has the essential role in antioxidant defence system.^{38, 39} Meanwhile, p53 also transactivates a serial of genes encoding proteins that promote intracellular ROS generation.^{40, 41} In p53-null H1299 cells, we observed the higher basal level of ROS when compared with A549 cells, indicating that p53 might play the important role in inhibiting oxidative stress in lung carcinoma. On the other hand, Polyak et al. first proposed a model in which p53-induced apoptosis is associated with the generation of cellular ROS mediated by PIGs, such as p53-induced gene 3 (PIG3) which is a homolog of NADPH:quinone oxidoreductase and has been implicated in p53-induced apoptosis.⁴¹ In the present study, we found that OH-GQDs didn't affect the expression level of PIG3. Consistent with this, we didn't find the effect of OH-GQDs on cells apoptosis (Data not shown). How OH-GQDs influence the p53-induced genes expression

profile and ultimately determine the fate of cells still remains unclear.

Sustained generation of ROS induces the intracellular oxidative stress which will eventually lead to cellular senescence through activating p21 signal pathway.⁴² The retinoblastoma protein (Rb) plays essential role in cellular senescence maintenance. The tumor suppressor Rb binds to the transcription factor E2F and blocks its interaction with target genes which function to facilitate G1/S cell cycle transition. The Cyclin/CDK mediated phosphorylation of Rb disrupts the binding of Rb to E2F,⁴³ allowing the promotion of normal cell cycle progression. p53-dependent or -independent p21 activation can inhibit cyclin/CDK activity and phosphorylation of Rb. Our data showed that OH-GQDs induce cellular senescence and the phosphorylation of Rb was suppressed in both lung carcinoma p53 wild-type A549 and p53 deficient H1299 cells. Altogether, our investigation demonstrated that nanomaterial OH-GQDs induce cell cycle arrest, senescence might via activating p21-Rb signal pathway in both p53-dependent and -independent pathway. Recently, Ulusoy and colleagues' work evaluated the cytotoxicity effects of CdTe/CdS/ZnS quantum dots on three-dimensional (3D) spheroid cultured human adipose-derived mesenchymal stem cells (hAD-MSCs).⁴⁴ It warrants further investigation to assess the cytotoxicity of OH-GQDs using the 3D in vitro model.

Conclusions

Our study indicated that hydroxyl-modified GQDs exhibits obvious cytotoxicity on lung carcinoma cells. OH-GQDs are able to regulate intracellular ROS generation and G0-G1 cell cycle arrest. In addition, hydroxylated GQDs treatment leads cellular senescence which might be mediated by activating p21-Rb signal pathway in both p53-dependent and -independent manner.

Conflicts of interest

There are no conflicts of interest to declare.

Acknowledgements

This work was supported by the National Natural Science Foundation of China (81530085, 81472919, 81573079), and the Natural Science Foundation of Jiangsu Province of China (BK20131149), the Six Talent Peaks Project of Jiangsu Province of China (WSN095), the Suzhou Administration of Science and Technology (SYS201360) and Suzhou Key Medical Center (SZZX201506).

References

- 1 J. H. Shen, Y. H. Zhu, X. L. Yang and C. Z. Li, Graphene quantum dots: emergent nanolights for bioimaging, sensors, catalysis and photovoltaic devices, *Chem Commun*, 2012, **48**, 3686-3699.

- 2 D. Y. Pan, J. C. Zhang, Z. Li and M. H. Wu, Hydrothermal Route for Cutting Graphene Sheets into Blue-Luminescent Graphene Quantum Dots, *Adv Mater*, 2010, **22**, 734-+.
- 3 Y. Li, Y. Hu, Y. Zhao, G. Q. Shi, L. E. Deng, Y. B. Hou and L. T. Qu, An Electrochemical Avenue to Green-Luminescent Graphene Quantum Dots as Potential Electron-Acceptors for Photovoltaics, *Adv Mater*, 2011, **23**, 776-+.
- 4 X. Yan, X. Cui, B. S. Li and L. S. Li, Large, Solution-Processable Graphene Quantum Dots as Light Absorbers for Photovoltaics, *Nano Lett*, 2010, **10**, 1869-1873.
- 5 X. T. Zheng, A. Than, A. Ananthanaraya, D. H. Kim and P. Chen, Graphene Quantum Dots as Universal Fluorophores and Their Use in Revealing Regulated Trafficking of Insulin Receptors in Adipocytes, *Acs Nano*, 2013, **7**, 6278-6286.
- 6 Z. M. Markovic, B. Z. Ristic, K. M. Arskin, D. G. Klisic, L. M. Harhaji-Trajkovic, B. M. Todorovic-Markovic, D. P. Kepic, T. K. Kravic-Stevovic, S. P. Jovanovic, M. M. Milenkovic, D. D. Milivojevic, V. Z. Bumbasirevic, M. D. Dramicanin and V. S. Trajkovic, Graphene quantum dots as autophagy-inducing photodynamic agents, *Biomaterials*, 2012, **33**, 7084-7092.
- 7 L. M. Zhang, Y. D. Xing, N. Y. He, Y. Zhang, Z. X. Lu, J. P. Zhang and Z. J. Zhang, Preparation of Graphene Quantum Dots for Bioimaging Application, *J Nanosci Nanotechno*, 2012, **12**, 2924-2928.
- 8 C. Wang, C. Y. Wu, X. J. Zhou, T. Han, X. Z. Xin, J. Y. Wu, J. Y. Zhang and S. W. Guo, Enhancing Cell Nucleus Accumulation and DNA Cleavage Activity of Anti-Cancer Drug via Graphene Quantum Dots, *Sci Rep-Uk*, 2013, **3**.
- 9 J. C. Qiu, R. B. Zhang, J. H. Li, Y. H. Sang, W. Tang, P. R. Gil and H. Liu, Fluorescent graphene quantum dots as traceable, pH-sensitive drug delivery systems, *Int J Nanomed*, 2015, **10**, 6709-6724.
- 10 J. C. Ge, M. H. Lan, B. J. Zhou, W. M. Liu, L. Guo, H. Wang, Q. Y. Jia, G. L. Niu, X. Huang, H. Y. Zhou, X. M. Meng, P. F. Wang, C. S. Lee, W. J. Zhang and X. D. Han, A graphene quantum dot photodynamic therapy agent with high singlet oxygen generation, *Nat Commun*, 2014, **5**.
- 11 Z. H. Wang, J. F. Xia, C. F. Zhou, B. Via, Y. Z. Xia, F. F. Zhang, Y. H. Li, L. H. Xia and J. Tang, Synthesis of strongly green-photoluminescent graphene quantum dots for drug carrier, *Colloid Surface B*, 2013, **112**, 192-196.
- 12 S. J. Zhu, J. H. Zhang, C. Y. Qiao, S. J. Tang, Y. F. Li, W. J. Yuan, B. Li, L. Tian, F. Liu, R. Hu, H. N. Gao, H. T. Wei, H. Zhang, H. C. Sun and B. Yang, Strongly green-photoluminescent graphene quantum dots for bioimaging applications, *Chem Commun*, 2011, **47**, 6858-6860.
- 13 L. Z. Feng and Z. A. Liu, Graphene in biomedicine: opportunities and challenges, *Nanomedicine-Uk*, 2011, **6**, 317-324.
- 14 C. Y. Wu, C. Wang, T. Han, X. J. Zhou, S. W. Guo and J. Y. Zhang, Insight into the Cellular Internalization and Cytotoxicity of Graphene Quantum Dots, *Adv Healthc Mater*, 2013, **2**, 1613-1619.
- 15 Y. Chong, Y. F. Ma, H. Shen, X. L. Tu, X. Zhou, J. Y. Xu, J. W. Dai, S. J. Fan and Z. J. Zhang, The in vitro and in vivo toxicity of graphene quantum dots, *Biomaterials*, 2014, **35**, 5041-5048.
- 16 Y. R. Qin, Z. W. Zhou, S. T. Pan, Z. X. He, X. J. Zhang, J. X. Qiu, W. Duan, T. X. Yang and S. F. Zhou, Graphene quantum dots induce apoptosis, autophagy, and inflammatory response via p38 mitogen-activated protein kinase and nuclear factor-kappa B mediated signaling pathways in activated THP-1 macrophages, *Toxicology*, 2015, **327**, 62-76.
- 17 S. M. Zhang, Z. F. Shang and P. K. Zhou, Autophagy as the effector and player in DNA damage response of cells to genotoxicants, *Toxicol Res-Uk*, 2015, **4**, 613-622.
- 18 D. Wang, L. Zhu, J. F. Chen and L. M. Dai, Can graphene quantum dots cause DNA damage in cells?, *Nanoscale*, 2015, **7**, 9894-9901.
- 19 S. Matt and T. G. Hofmann, The DNA damage-induced cell death response: a roadmap to kill cancer cells, *Cellular and molecular life sciences : CMLS*, 2016, DOI: 10.1007/s00018-016-2130-4.
- 20 M. Zhao, F. Yang, Y. Xue, D. Xiao and Y. Guo, Effects of edge oxidation on the stability and half-metallicity of graphene quantum dots, *Chemphyschem : a European journal of chemical physics and physical chemistry*, 2014, **15**, 157-164.
- 21 X. Yuan, Z. Liu, Z. Guo, Y. Ji, M. Jin and X. Wang, Cellular distribution and cytotoxicity of graphene quantum dots with different functional groups, *Nanoscale research letters*, 2014, **9**, 108.
- 22 T. T. Wang, S. J. Zhu and X. E. Jiang, Toxicity mechanism of graphene oxide and nitrogen-doped graphene quantum dots in RBCs revealed by surface-enhanced infrared absorption spectroscopy, *Toxicol Res-Uk*, 2015, **4**, 885-894.
- 23 L. Yu, Z. F. Shang, F. M. Hsu, Z. Zhang, V. Tumati, Y. F. Lin, B. P. C. Chen and D. Saha, NSCLC cells demonstrate differential mode of cell death in response to the combined treatment of radiation and a DNA-PKcs inhibitor, *Oncotarget*, 2015, **6**, 3848-3860.
- 24 L. H. Zou, Z. F. Shang, W. Tan, X. D. Liu, Q. Z. Xu, M. Song, Y. Wang, H. Guan, S. M. Zhang, L. Yu, C. G. Zhong and P. K. Zhou, TNKS1BP1 functions in DNA double-strand break repair through facilitating DNA-PKcs autophosphorylation dependent on PARP-1, *Oncotarget*, 2015, **6**, 7011-7022.
- 25 Z. F. Shang, B. Huang, Q. Z. Xu, S. M. Zhang, R. Fan, X. D. Liu, Y. Wang and P. K. Zhou, Inactivation of DNA-Dependent Protein Kinase Leads to Spindle Disruption and Mitotic Catastrophe with Attenuated Checkpoint Protein 2 Phosphorylation in Response to DNA Damage, *Cancer research*, 2010, **70**, 3657-3666.
- 26 G. S. Jimenez, S. H. Khan, J. M. Stommel and G. M. Wahl, p53 regulation by post-translational modification and nuclear retention in response to diverse stresses, *Oncogene*, 1999, **18**, 7656-7665.
- 27 Q. Li, R. R. Falsey, S. Gaitonde, V. Sotello, K. Kislin and J. D. Martinez, Genetic analysis of p53 nuclear importation, *Oncogene*, 2007, **26**, 7885-7893.
- 28 K. T. Biegging, S. S. Mello and L. D. Attardi, Unravelling mechanisms of p53-mediated tumour suppression, *Nature reviews. Cancer*, 2014, **14**, 359-370.
- 29 J. H. An, S. M. Jang, J. W. Kim, C. H. Kim, P. I. Song and K. H. Choi, The expression of p21 is upregulated by forkhead box A1/2 in p53-null H1299 cells, *FEBS letters*, 2014, **588**, 4065-4070.
- 30 C. M. Aliouat-Denis, N. Dendouga, I. Van den Wyngaert, H. Goehlmann, U. Steller, I. van de Weyer, N. Van Slycken, L. Andries, S. Kass, W. Luyten, M. Janicot and J. E. Vialard, p53-independent regulation of p21Waf1/Cip1 expression and senescence by Chk2, *Molecular cancer research : MCR*, 2005, **3**, 627-634.
- 31 A. L. Gartel, E. Goufman, F. Najmabadi and A. L. Tyner, Sp1 and Sp3 activate p21 (WAF1/CIP1) gene transcription in the Caco-2 colon adenocarcinoma cell line, *Oncogene*, 2000, **19**, 5182-5188.
- 32 R. Ju and M. T. Muller, Histone deacetylase inhibitors activate p21(WAF1) expression via ATM, *Cancer research*, 2003, **63**, 2891-2897.
- 33 K. Somasundaram, H. Zhang, Y. X. Zeng, Y. Houvras, Y. Peng, G. S. Wu, J. D. Licht, B. L. Weber and W. S. El-Deiry, Arrest of the cell cycle by the tumour-suppressor BRCA1 requires the CDK-inhibitor p21WAF1/CIP1, *Nature*, 1997, **389**, 187-190.

- 34 H. Li and X. Wu, Histone deacetylase inhibitor, Trichostatin A, activates p21WAF1/CIP1 expression through downregulation of c-myc and release of the repression of c-myc from the promoter in human cervical cancer cells, *Biochemical and biophysical research communications*, 2004, **324**, 860-867.
- 35 I. Dutto, M. Tillhon, O. Cazzalini, L. A. Stivala and E. Prosperi, Biology of the cell cycle inhibitor p21(CDKN1A): molecular mechanisms and relevance in chemical toxicology, *Archives of toxicology*, 2015, **89**, 155-178.
- 36 Y. Ye, J. Liu, M. Chen, L. Sun and M. Lan, In vitro toxicity of silica nanoparticles in myocardial cells, *Environmental toxicology and pharmacology*, 2010, **29**, 131-137.
- 37 R. Roy, S. K. Singh, L. K. Chauhan, M. Das, A. Tripathi and P. D. Dwivedi, Zinc oxide nanoparticles induce apoptosis by enhancement of autophagy via PI3K/Akt/mTOR inhibition, *Toxicology letters*, 2014, **227**, 29-40.
- 38 S. P. Hussain, P. Amstad, P. He, A. Robles, S. Lupold, I. Kaneko, M. Ichimiya, S. Sengupta, L. Mechanic, S. Okamura, L. J. Hofseth, M. Moake, M. Nagashima, K. S. Forrester and C. C. Harris, p53-induced up-regulation of MnSOD and GPx but not catalase increases oxidative stress and apoptosis, *Cancer research*, 2004, **64**, 2350-2356.
- 39 M. Tan, S. Li, M. Swaroop, K. Guan, L. W. Oberley and Y. Sun, Transcriptional activation of the human glutathione peroxidase promoter by p53, *The Journal of biological chemistry*, 1999, **274**, 12061-12066.
- 40 M. Y. Kang, H. B. Kim, C. Piao, K. H. Lee, J. W. Hyun, I. Y. Chang and H. J. You, The critical role of catalase in prooxidant and antioxidant function of p53, *Cell death and differentiation*, 2013, **20**, 117-129.
- 41 K. Polyak, Y. Xia, J. L. Zweier, K. W. Kinzler and B. Vogelstein, A model for p53-induced apoptosis, *Nature*, 1997, **389**, 300-305.
- 42 N. E. Sharpless and C. J. Sherr, Forging a signature of in vivo senescence, *Nature Reviews Cancer*, 2015, **15**, 397-408.
- 43 A. M. Narasimha, M. Kaulich, G. S. Shapiro, Y. J. Choi, P. Sicinski and S. F. Dowdy, Cyclin D activates the Rb tumor suppressor by mono-phosphorylation, *Elife*, 2014, **3**.
- 44 M. Ulusoy, A. Lavrentieva, J. G. Walter, F. Sambale, M. Green, F. Stahl and T. Scheper, Evaluation of CdTe/CdS/ZnS core/shell/shell quantum dot toxicity on three-dimensional spheroid cultures, *Toxicol Res-Uk*, 2016, **5**, 126-135.

OH-GQDs exhibit obvious cytotoxicity on lung carcinoma cells via inducing cells senescence in both p53-dependent and -independent manner.

